



Slowly rotating quantum dust cores and black holes

R. Casadio^{1,2,a} , L. Tabarroni^{1,b}

¹ Dipartimento di Fisica e Astronomia “A. Righi”, Università di Bologna, via Iriero 46, 40126 Bologna, Italy

² I.N.F.N., Sezione di Bologna, I.S. FLAG, viale B. Pichat 6/2, 40127 Bologna, Italy

Received: 13 December 2022 / Accepted: 14 January 2023
© The Author(s) 2023

Abstract We study the effect of rotation on the spectrum of bound states for dust cores that source (quantum) black holes found in Eur. Phys. J. C 82 (2022) 10. The dust ball is assumed to spin rigidly with sufficiently slow angular velocity that perturbation theory can be applied. Like the total mass, the total angular momentum is shown to be quantised in Planck units, hence so is the horizon area. For sufficiently small fraction of mass in the outermost layer, the model admits ground states which can spin fast enough within the perturbative regime so as to describe regular rotating objects rather than black holes.

1 Introduction

Many proposals for resolving the classical spacetime singularities [1] in approaches to quantum gravity have been put forward (for a necessarily limited selection, see Refs. [2–7]). Quite remarkably, a general feature obtained in semiclassical models of the gravitational collapse is the appearance of a bounce at a minimum radius [8–10], which suggests that understanding the dynamics of matter in the description of black hole formation [11] (and subsequent evolution [12]) is crucial. However, the nonlinearity of Einstein’s equations makes it impossible to study realistic classical models analytically, and this furthermore renders their quantum description intractable in general.

One can still hope to make some progress by studying those (over)simplified models obtained by forcing a strong symmetry and unphysical equations of state for the collapsing matter which are employed to solve the Einstein equations at the classical level. One such example is given by the Oppenheimer and Snyder model of a ball of dust collapsing solely under its own weight [13]. A discrete spectrum of bound states for this prototype of matter core was found in Ref. [14] (see also Ref. [15] for more results¹) for which we will here estimate the effect of rotation. The key idea in Ref. [14] was to quantise the radial geodesic equation for dust located at the areal radius of the ball in the Schwarzschild spacetime as an effective quantum mechanical description of the outermost layer. In order to deal with rotation, we shall here include the term in that geodesic equation containing the angular momentum for a rigidly rotating ball and compute its perturbative effects on the spectrum for sufficiently slow angular velocity.

2 Core quantum spectrum

Let us start by considering the collapse of a perfectly isotropic ball of dust with total ADM mass [21] M and areal radius $R = R(\tau)$. Here τ is the proper time of the dust particles following radial geodesics $r = r(\tau)$ in the Schwarzschild spacetime metric²

$$ds^2 = -\left(1 - \frac{2G_N M_0}{r}\right) dt^2 + \left(1 - \frac{2G_N M_0}{r}\right)^{-1} dr^2 + r^2(d\theta^2 + \sin^2\theta d\phi^2) \quad (2.1)$$

where $M_0 = M_0(r)$ is the (constant) fraction of ADM mass inside the sphere of radius $r = r(\tau)$.

¹ For thin shells, see Refs. [16–20].

² We shall always use units with $c = 1$ and often write the Planck constant $\hbar = \ell_P m_P$ and the Newton constant $G_N = \ell_P / m_P$, where ℓ_P and m_P are the Planck length and mass, respectively.

^a e-mail: casadio@bo.infn.it (corresponding author)

^b e-mail: luca.tabarroni@studio.unibo.it

In particular, we consider the outermost (thin) layer of (average) radius $r = R(\tau)$ and mass $\mu = \epsilon M$, where $0 < \epsilon < 1$ is the fraction of mass in that layer.³ The evolution of R is governed by the mass-shell condition for the massive layer of four-velocity $u^\alpha = (\dot{t}, \dot{R}, 0, 0)$, that is

$$\frac{E_\mu^2}{\mu^2} - \dot{R}^2 + \frac{2 G_N M_0}{R} - \left(1 - \frac{2 G_N M_0}{R}\right) \frac{L_\mu^2}{R^2 \mu^2} = 1 \tag{2.2}$$

where dots denote derivatives with respect to τ , $M_0 = (1 - \epsilon) M$, and E_μ and L_μ are the conserved momenta conjugated to $t = t(\tau)$ and $\phi = \phi(\tau)$, respectively.

2.1 Zero angular momentum and mass quantisation

The case of purely radial motion was analysed in Refs. [14, 15], which we briefly review here. For $L_\mu = 0$, Eq. (2.2) reads

$$H_0 \equiv \frac{P^2}{2 \epsilon M} - \frac{\epsilon(1 - \epsilon) G_N M^2}{R} = \frac{\epsilon M}{2} \left(\frac{E_\mu^2}{\epsilon^2 M^2} - 1 \right) \equiv \mathcal{E} \tag{2.3}$$

where $P = \epsilon M \dot{R}$ is the momentum conjugated to $R = R(\tau)$. The canonical quantisation prescription with $\hat{P} = -i \hbar \partial_R$ allows us to write Eq. (2.3) as the time-independent Schrödinger equation

$$\hat{H}_0 \Psi_{\bar{n}} = \left[-\frac{\hbar^2}{2 \epsilon M} \left(\frac{d^2}{dR^2} + \frac{2}{R} \frac{d}{dR} \right) - \frac{\epsilon(1 - \epsilon) G_N M^2}{R} \right] \Psi_{\bar{n}} = \mathcal{E}_{\bar{n}} \Psi_{\bar{n}} \tag{2.4}$$

which is formally the same as the one for the s -states of the hydrogen atom. The solutions are thus given by the Hamiltonian eigenfunctions

$$\Psi_{\bar{n}}(R) = \sqrt{\frac{\epsilon^6 (1 - \epsilon)^3 M^9}{\pi \ell_p^3 m_p^9 \bar{n}^5}} \exp\left(-\frac{\epsilon^2 (1 - \epsilon) M^3 R}{\bar{n} m_p^3 \ell_p}\right) L_{\bar{n}-1}^1\left(\frac{2 \epsilon^2 (1 - \epsilon) M^3 R}{\bar{n} m_p^3 \ell_p}\right) \tag{2.5}$$

where the normalisation is defined in the scalar product

$$\langle \bar{n} | \bar{n}' \rangle = 4 \pi \int_0^\infty R^2 \Psi_{\bar{n}}^*(R) \Psi_{\bar{n}'}(R) dR = \delta_{\bar{n}\bar{n}'} \tag{2.6}$$

the functions $L_{\bar{n}-1}^1$ are Laguerre polynomials and the nonnegative integer quantum number \bar{n} corresponds to the eigenvalues

$$\mathcal{E}_{\bar{n}} = -\frac{\epsilon^3 (1 - \epsilon)^2 M^5}{2 \bar{n}^2 m_p^4}. \tag{2.7}$$

The expectation value of the areal radius on these states is given by

$$\bar{R}_{\bar{n}} \equiv \langle \bar{n} | \hat{R} | \bar{n} \rangle = \frac{3 \ell_p \bar{n}^2 m_p^3}{2 \epsilon^2 (1 - \epsilon) M^3} \tag{2.8}$$

so that the quantum picture is the same that one would have in Newtonian physics. In particular, the ground state $\bar{n} = 1$ has a width $\bar{R}_1 \sim \ell_p (m_p/M)^3$ and energy $\mathcal{E}_1 \sim -M (M/m_p)^4$, which makes it practically indistinguishable from a point-like singularity if $M \gg m_p$.

In fact, the only general relativistic feature that the model retains is given by $\mathcal{E} = \mathcal{E}(E_\mu)$ in Eq. (2.3). By then assuming that E_μ is well defined for the allowed quantum states, we obtain

$$0 \leq \frac{E_\mu^2}{\epsilon^2 M^2} = 1 - \frac{\epsilon^2 (1 - \epsilon)^2}{\bar{n}^2} \left(\frac{M}{m_p}\right)^4 \tag{2.9}$$

which yields the lower bound

$$\bar{n} \geq N_M \equiv \epsilon (1 - \epsilon) \left(\frac{M}{m_p}\right)^2. \tag{2.10}$$

The fundamental state of the outermost layer hence corresponds to $\bar{n} = N_M \gg 1$, with

$$\mathcal{E}_{N_M} = -\frac{\epsilon M}{2}. \tag{2.11}$$

³ See Ref. [15] for more details about the role of ϵ .

This result clearly resembles Bekenstein’s famous area law quantisation [22], since the allowed values of the mass and gravitational area are quantised in Planck units according to ⁴

$$\mathcal{A}_M = 16 \pi G_N^2 M^2 = \frac{16 \ell_p^2 N_M}{\epsilon (1 - \epsilon)} \tag{2.12}$$

where the entire spectrum is given by $\bar{n} = N_M + n$, with n a nonnegative integer.

We can now see that the singularity is precluded, as one expects from semiclassical models [8, 9], since

$$\bar{R}_{N_M} = \frac{3}{2} (1 - \epsilon) G_N M = \frac{3}{4} (1 - \epsilon) R_H \tag{2.13}$$

and $\bar{R}_{N_M} \sim R_H \gg \ell_p$ unless the value of ϵ is extremely close to 1. Furthermore $\bar{R}_{N_M} < (3/4) R_H$ for any value of $0 < \epsilon < 1$, so that a non-spinning dust ball in the ground state can be the matter core of a quantum black hole for any mass M . We also notice that the relative uncertainty in the areal radius is given by

$$\frac{\Delta R_{\bar{n}}}{\bar{R}_{\bar{n}}} \equiv \frac{\sqrt{\langle \bar{n} | \hat{R}^2 | \bar{n} \rangle - \bar{R}_{\bar{n}}^2}}{\bar{R}_{\bar{n}}} = \frac{\sqrt{\bar{n}^2 + 2}}{3 \bar{n}} \tag{2.14}$$

which asymptotes to a minimum of 1/3 for $\bar{n} \rightarrow \infty$. In the following, for simplicity, we will mostly consider the ground state $\bar{n} = N_M$ with $M \gg m_p$.⁵

2.2 Rigidly rotating ball

Next, we consider the case of a dust ball which rotates rigidly with angular velocity ω . A proper general relativistic treatment would require replacing the outer Schwarzschild geometry with the Kerr metric, but we will here be satisfied with a perturbative approach for the quantum system described previously. In particular, the outermost layer would have classical angular momentum

$$L_\epsilon = \frac{2}{3} \epsilon M R^2 \omega \tag{2.15}$$

which we assume is small enough and replace for L_μ in Eq. (2.2). This yields the total Hamiltonian $H = H_0 + V_L$, where H_0 is given in Eq. (2.3) and

$$\begin{aligned} V_L &= \left(1 - \frac{2 G_N (1 - \epsilon) M}{R} \right) \frac{L_\epsilon^2}{2 \epsilon M R^2} \\ &= \frac{2}{9} \epsilon M [R^2 - 2 G_N (1 - \epsilon) M R] \omega^2. \end{aligned} \tag{2.16}$$

In perturbation theory, this term will result in a correction to the eigenvalues (2.7) given by

$$\Delta \mathcal{E}_{\bar{n}} \equiv \langle \bar{n} | \hat{V}_L | \bar{n} \rangle \simeq \frac{2}{9} \epsilon M \bar{R}_{\bar{n}} \left[\frac{10}{9} \bar{R}_{\bar{n}} - 2 G_N (1 - \epsilon) M \right] \omega^2 \tag{2.17}$$

where we used Eq. (2.14) for $\bar{n} \gg 1$ and $\bar{R}_{\bar{n}}$ is given in Eq. (2.8).

For the ground state $\bar{n} = N_M$, we thus find

$$\begin{aligned} \Delta \mathcal{E}_{N_M} &\simeq \frac{m_p^4 - \epsilon^2 (1 - \epsilon)^2 M^4}{9 \epsilon M} G_N^2 \omega^2 \\ &\simeq -\frac{1}{9} \epsilon M (1 - \epsilon)^2 G_N^2 M^2 \omega^2 \end{aligned} \tag{2.18}$$

in which we assumed that $\epsilon (1 - \epsilon) M^2 \gg m_p^2$. We then have

$$\langle N_M | \hat{H} | N_M \rangle = \mathcal{E}_{N_M} + \Delta \mathcal{E}_{N_M} \simeq \mathcal{E}_{N_M} \left[1 + \frac{2}{9} (1 - \epsilon)^2 G_N^2 M^2 \omega^2 \right]. \tag{2.19}$$

This result is acceptable as long as $|\Delta \mathcal{E}_{N_M}| \ll |\mathcal{E}_{N_M}|$, or

$$|\omega| \ll \frac{3}{\sqrt{2} (1 - \epsilon) G_N M} \equiv \omega_{\max} \tag{2.20}$$

We further notice that ω_{\max} corresponds to a total angular momentum per unit mass given by

$$a_{\max} \equiv \frac{L_c}{M} = \frac{2}{5} \langle N_M | \hat{R}^2 | N_M \rangle \omega_{\max} \simeq 2 (1 - \epsilon) G_N M. \tag{2.21}$$

⁴ We recall that $R_H = 2 G_N M$ is the classical Schwarzschild (or gravitational) radius of the ball.

⁵ For instance, for $M = M_\odot \simeq 10^{30}$ kg, one finds $N_M \sim 10^{76}$.

In the same approximation, we can compute the correction to the ground state quantum number to leading order in ω , which is given by

$$N_{ML} \simeq N_M \left[1 + \frac{1}{9} (1 - \epsilon)^2 G_N^2 M^2 \omega^2 \right]. \quad (2.22)$$

As expected, the angular momentum acts as an effective potential barrier and increases the minimum allowed quantum number from N_M to N_{ML} , corresponding to a larger radius

$$\bar{R}_{N_{ML}} \simeq \bar{R}_{N_M} \left[1 + \frac{2}{9} (1 - \epsilon)^2 G_N^2 M^2 \omega^2 \right]. \quad (2.23)$$

In particular, for $\omega = \omega_{\max}$, one obtains

$$N_{\max} = \frac{3}{2} \epsilon (1 - \epsilon) \left(\frac{M}{m_p} \right)^2 = \frac{3}{2} N_M \quad (2.24)$$

corresponding to a radius $\bar{R}_{\max} = 2 \bar{R}_{N_M} = 3(1 - \epsilon) G_N M$.

2.3 Outer geometry

We can now study the geometry outside the ball in the ground state by assuming that it is indeed given by the Kerr metric. We recall that the outer horizon for a Kerr metric is located at

$$\begin{aligned} R_+ &= G_N M + \sqrt{G_N^2 M^2 - a^2} \\ &\simeq 2 G_N M \left[1 - \frac{1}{4} (1 - \epsilon)^4 G_N^2 M^2 \omega^2 \right] \end{aligned} \quad (2.25)$$

whereas the inner Cauchy horizon would be at

$$\begin{aligned} R_- &= G_N M - \sqrt{G_N^2 M^2 - a^2} \\ &\simeq \frac{1}{2} (1 - \epsilon)^4 G_N^3 M^3 \omega^2 \ll \bar{R}_{N_M}. \end{aligned} \quad (2.26)$$

Since R_- is located well inside the dust core, the relevant geometry will differ from the Kerr vacuum there and the inner horizon cannot be realised (at least) within the perturbative approximation. On the other hand, R_+ is larger than the core for

$$|\omega| < \omega_H = \sqrt{\frac{3 + 9\epsilon}{(1 - \epsilon)^3 (5 - 3\epsilon)}} \frac{1}{G_N M} \quad (2.27)$$

which is approximately equal to ω_{\max} in Eq. (2.20) for $\epsilon \simeq 0.5$ (see Fig. 1). The inner matter core approaches the outer horizon radius R_+ for $\omega \simeq \omega_H$, with $\omega_H < \omega_{\max}$ for $0 < \epsilon \lesssim 0.5$ and $\omega_H > \omega_{\max}$ for $0.5 \lesssim \epsilon < 1$. In general, it would seem that one can consider small enough values of ω so that the outer horizon is realised. Moreover, for sufficiently small ϵ , one can also describe cores that spin fast enough, so as not to form a black hole, within the perturbative regime. We will come back to this point in the following.

2.4 Angular momentum quantisation

In the above analysis, we considered the angular velocity ω as a (free) perturbative parameter, but Eq. (2.22) implies the necessary quantisation of the angular momentum. In fact, both N_M and N_{ML} must be (positive) integers in order to correspond to allowed states in the spectrum (2.5). This implies that $N_{ML} = N_M + n$, with n a (nonnegative) integer (much smaller than N_M for the perturbative result to hold), and we can write

$$\omega^2 \simeq \omega_n^2 = \frac{9\epsilon n}{(1 - \epsilon) N_M^2 \ell_p^2} \quad (2.28)$$

corresponding to a quantised angular momentum

$$L_n = \frac{3}{\epsilon} \ell_p m_p \sqrt{N_M n} \quad (2.29)$$

or

$$a_n \equiv \frac{L_n}{M} = 3 \ell_p \sqrt{\frac{1 - \epsilon}{\epsilon}} n \quad (2.30)$$

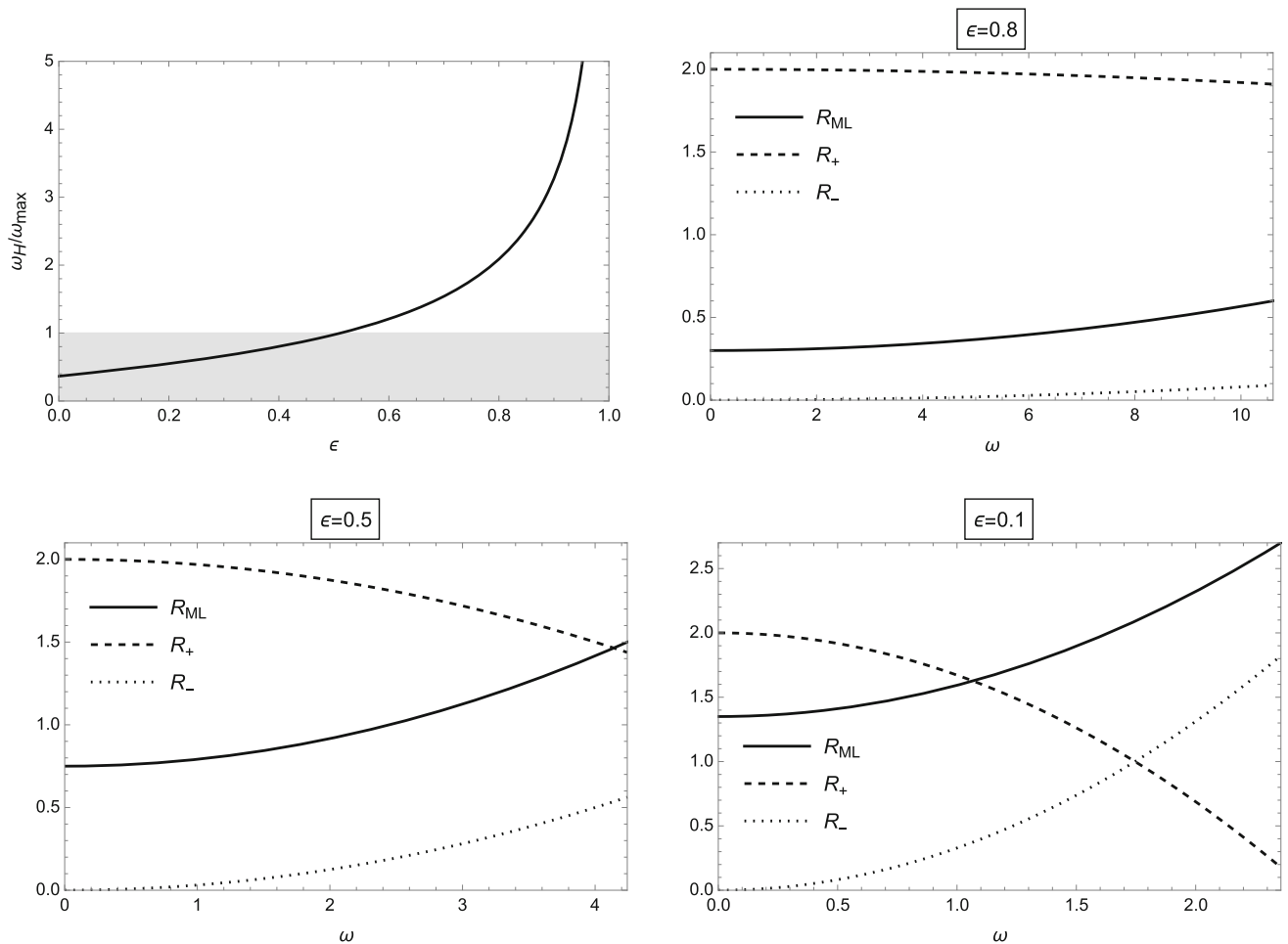


Fig. 1 Top left panel: ratio ω_H/ω_{\max} for $0 < \epsilon < 1$ (shaded area corresponds to $\omega_H < \omega_{\max}$). Top right to bottom left panels: core radius (solid line), outer horizon radius (dashed line) and inner horizon radius (dotted line) for $0 < \omega < \omega_{\max}(\epsilon)$ with $\epsilon = 0.8, 0.5$ and 0.1 (all quantities in units of $G_N M$)

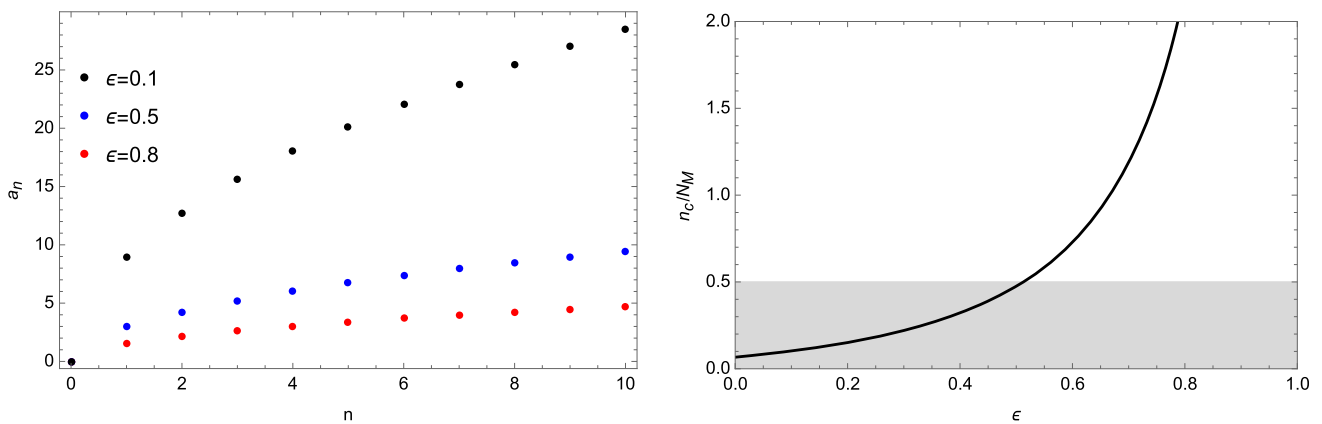


Fig. 2 Left panel: angular momentum-to-mass ratio (2.30) (in units of ℓ_p). Right panel: ratio n_c/N_M in Eq. (3.1) (shaded region marks the perturbative regime)

which is plotted in the left panel of Fig. 2 for a first few values of n and the same values of ϵ used in Fig. 1. Note that the condition (2.20) of small angular velocity then simply yields $n \ll N_M/2 \sim N_M$.

We can further notice that the quantisation of the mass and angular momentum lead to a quantisation of the outer horizon radius (2.25) and area in Planck units, namely

$$\mathcal{A}_+ = 4\pi R_+^2 \simeq \mathcal{A}_M \left[1 - \frac{9}{2} (1 - \epsilon)^2 \frac{n}{N_M} \right] \tag{2.31}$$

where \mathcal{A}_M is the horizon area (2.12) for a Schwarzschild black hole of mass M . We then see that increasing the mass (that is N_M) makes the horizon larger, whereas increasing the angular momentum (that is n) makes it smaller, consistently with the classical theory.

3 Final remarks

We have considered the perturbation induced by rotation on the quantum spectrum of dust balls found in Ref. [14]. Quite expectedly, we have found that adding angular momentum increases the size of the ground state. Moreover, no inner Cauchy horizon can appear within the perturbative regime, and the event horizon area (2.31) is now quantised in terms of two quantum numbers, namely $\bar{n} = N_M$ corresponding to the total mass M and n for the quantised total angular momentum of the system.

Increasing N_M makes both core and horizon larger, whereas increasing n makes the core larger but the event horizon smaller. There is therefore a critical angular velocity $\omega_{n_c} \simeq \omega_H$, that is

$$\frac{n_c}{N_M} \simeq \frac{1 + 3\epsilon}{3(1 - \epsilon)(5 - 3\epsilon)} \quad (3.1)$$

above which the core remains larger than the (would be outer) horizon and the system is not a black hole. From the right panel of Fig. 2, we see that this can occur within the perturbative regime if $0 < \epsilon \lesssim 0.5$, consistently with the top left panel of Fig. 1. An example is provided by the bottom right panel of Fig. 1, where $\epsilon = 0.1$ and the transition from a rotating black hole to a horizonless compact object occurs for $G_N M \omega \simeq 1$. Of course, beside the qualitative behaviour, the precise values obtained from such a simple model should not be trusted to bear a phenomenological relevance.

Acknowledgements R.C. is partially supported by the INFN grant FLAG and his work has also been carried out in the framework of activities of the National Group of Mathematical Physics (GNFM, INdAM).

Funding Open access funding provided by Alma Mater Studiorum - Università di Bologna within the CRUI-CARE Agreement.

Data Availability Statement Data sharing is not applicable to this article as no datasets were generated or analysed during the current study.

Open Access This article is licensed under a Creative Commons Attribution 4.0 International License, which permits use, sharing, adaptation, distribution and reproduction in any medium or format, as long as you give appropriate credit to the original author(s) and the source, provide a link to the Creative Commons licence, and indicate if changes were made. The images or other third party material in this article are included in the article's Creative Commons licence, unless indicated otherwise in a credit line to the material. If material is not included in the article's Creative Commons licence and your intended use is not permitted by statutory regulation or exceeds the permitted use, you will need to obtain permission directly from the copyright holder. To view a copy of this licence, visit <http://creativecommons.org/licenses/by/4.0/>.

References

1. S.W. Hawking, G.F.R. Ellis, *The Large Scale Structure of Space-Time* (Cambridge University Press, Cambridge, 1973)
2. P. Hajicek, C. Kiefer, Int. J. Mod. Phys. D **10**, 775 (2001). [arXiv:gr-qc/0107102 [gr-qc]]
3. I. Kuntz, R. Casadio, Phys. Lett. B **802**, 135219 (2020). [arXiv:1911.05037 [hep-th]]
4. I. Kuntz, Eur. Phys. J. C **78**, 3 (2018). [arXiv:1712.06582 [gr-qc]]
5. H.M. Haggard, C. Rovelli, Phys. Rev. D **92**, 104020 (2015). [arXiv:1407.0989 [gr-qc]]
6. I. Kuntz, R. da Rocha, Eur. Phys. J. C **79**, 447 (2019). [arXiv:1903.10642 [hep-th]]
7. W. Piechocki, T. Schmitz, Phys. Rev. D **102**, 046004 (2020). [arXiv:2004.02939 [gr-qc]]
8. V.P. Frolov, G.A. Vilkovisky, Phys. Lett. B **106**, 307 (1981)
9. R. Casadio, Int. J. Mod. Phys. D **9**, 511 (2000). [arXiv:gr-qc/9810073 [gr-qc]]
10. T. Schmitz, Phys. Rev. D **103**, 064074 (2021). [arXiv:2012.04383 [gr-qc]]
11. R. Casadio, A. Giugno, A. Giusti, Phys. Lett. B **763**, 337 (2016). [arXiv:1606.04744 [hep-th]]
12. R. Casadio, A. Giusti, Phys. Lett. B **797**, 134915 (2019). [arXiv:1904.12663 [gr-qc]]
13. J.R. Oppenheimer, H. Snyder, Phys. Rev. **56**, 455 (1939)
14. R. Casadio, Eur. Phys. J. C **82**, 10 (2022). [arXiv:2103.14582 [gr-qc]]
15. R. Casadio, R. da Rocha, P. Meert, L. Tabarroni, W. Barreto, "Configurational entropy of black hole quantum cores," [arXiv:2206.10398 [gr-qc]]
16. C. Vaz, Phys. Rev. D **105**, 086020 (2022). [arXiv:2204.02435 [gr-qc]]
17. P. Hajicek, B.S. Kay, K.V. Kuchar, Phys. Rev. D **46**, 5439 (1992)
18. P. Hajicek, C. Kiefer, Int. J. Mod. Phys. D **10**, 775 (2001). [arXiv:gr-qc/0107102 [gr-qc]]
19. R. Casadio, G. Venturi, Class. Quant. Grav. **13**, 2715 (1996). [arXiv:gr-qc/9512032 [gr-qc]]
20. V. Husain, J.G. Kelly, R. Santacruz, E. Wilson-Ewing, Phys. Rev. Lett. **128**, 121301 (2022). [arXiv:2109.08667 [gr-qc]]
21. R.L. Arnowitt, S. Deser, C.W. Misner, Phys. Rev. **116**, 1322 (1959)
22. J.D. Bekenstein, Phys. Rev. D **7**, 2333 (1973)